International Journal of Mechanical, Industrial and Aerospace Sciences
ISSN: 2517-9950
Vol:2, No:4, 2008

The Comparison of Form Drag and Profile Drag of a Wind Turbine Blade Section in Pitching Oscillation

M. R. Soltani, M. Seddighi, and M. Mahmoudi

***Abstract*—**Extensive wind tunnel tests have been conducted to investigate the unsteady flow field over and behind a 2D model of a 660 kW wind turbine blade section in pitching motion. The surface pressure and wake dynamic pressure variation at a distance of 1.5 chord length from trailing edge were measured by pressure transducers during several oscillating cycles at 3 reduced frequencies and oscillating amplitudes. Moreover, form drag and linear momentum deficit are extracted and compared at various conditions. The results show that the wake velocity field and surface pressure of the model have similar behavior before and after the airfoil beyond the static stall angle of attack. In addition, the effects of reduced frequency and oscillation amplitudes are discussed.

***Keywords*—**Pitching motion, form drag, Profile drag, wind turbine.

I. Introduction

AERODYNAMIC bodies or lifting surfaces subjected to time-dependent unsteady motion histories elicit unsteady boundary-layer behavior, separation, and in severe maneuvers, dynamic stall and dynamic reattachment. Because of their complicated, rapidly changing time dependent nature, significant amount of research both theoretical and experimental has been conducted to understand the fluid mechanics of these flow fields. From the classical lifting line theory after the flow starts on a fixed airfoil, to satisfy the boundary conditions on the airfoil surface, the vorticity around the airfoil must be increased. On the other hand, Kelvin's theory implies that equal amount of vorticity but in opposite sign sheds into the wake. Once the steady state is reached, the net amount of vorticity sheds into the wake over a finite time is zero and the circulation around the airfoil becomes constant. In the case of oscillating airfoils, because of time variation of surface boundary conditions, the bound circulation around the airfoil varies with time, therefore the vortices and the structure of the wake must follow these variations. The temporal and spatial evolution of these structures dominates the unsteady flow behavior over the airfoil. They can induce considerable lift increase or trigger a catastrophic flow breakdown when they detach from the surface.

Theoretical studies for incompressible, unsteady airfoil problems have been formulated in both the frequency domain and the time-domain, primarily by Wagner, Theodorsen, Kussner, and Von Karman & Sears. An authoritative source documenting these classical theories is Bisplinghoff et al., with further details of their application given by Leishman. These formulations have the same root in unsteady thin-airfoil theory, and give exact analytic solutions for airloads for different forcing conditions, i.e., for airfoil motions or for externally imposed velocity fields [1, 2].

Recently considerable experimental research has been conducted into the problem of unsteady aerodynamics of oscillating airfoils. Most of them were directed to unsteady wing loading and dynamic stall process [3-8].

There are many practical situations were unsteady wakes are involved. The wake blade interaction in turbomachinary [9] and propulsive characteristics of flapping wings [10] are some examples.

Ho and Chen [11] studied experimentally the unsteady wake of a plunging airfoil by use of hot-wire rake. The velocity traces and the Reynolds-stress distributions in their study revealed that the wake had different turbulent structures in the upper and lower parts. Park, Kim and Lee [12] measure the velocity field in the wake of a NACA0012 airfoil by use of a hot wire probe traversing in the vertical direction. They showed that at a same instantaneous angle of attack during pitch up and pitch down motions of the airfoil, velocity and turbulence intensity profiles in the wake are different owing to the hysteresis or time history of the flow. Koochesfahani [13] studied the vortical patterns in the wake of a NACA0012 oscillating airfoil at a very low speed flow in a water tunnel and showed that the oscillation wave form has an important effect in the vortical pattern shapes and mean velocity profiles in the wake. He found there is a critical value for oscillation frequency that the usual velocity defect profiles in the wake changes to excessive momentum profile like a jet flow and the airfoil produces trust force. Panda and Zaman [14] studied the wake of an oscillating NACA0012 airfoil at mean angle of attacks above the static stall angle by use of hot wire anemometry and flow visualization and saw that in addition to the familiar dynamic stall vortex (DSV), an intense vortex of

M. R. Soltani, Professor, is with Aerospace Engineering Department, Sharif University of Technology, Tehran, Iran (e-mail: msoltani@sharif.edu).
M. Seddighi is with Department of Mechanical Engineering, University of Aberdeen, Aberdeen, UK (e-mail: seddighi@abdn.ac.uk).
M. Mahmoudi is with Aerospace Engineering Department, Sharif University of Technology, Tehran, Iran (e-mail: mahmoudi.mohamad@gmail.com).

opposite sign originates from the trailing edge just when the DSV is shed. The two together take the shape of the cross section of a large mushroom. They also measure the flux of vorticity shed into the wake and compute the circulatory part of the lift coefficient by the Kutta-Jukovskey theory and also measure the convection velocity in the wake. They found that the average wake convection velocity is independent of reduced frequency but it decreases with increasing the mean angle of attack and amplitude of oscillation.

Wind turbines operate for most of their time in an unsteady flow environment. The blade element forces vary in time and space as a result of ambient turbulence, persistent shear in the ambient wind, blade vibratory motions, control inputs, and skewed flow. The analysis of horizontal axis wind turbine (HAWT) blade loads is subdivided into two major areas: dynamic stall and dynamic inflow [15-18].

Wind turbine airfoils operate frequently under fully separated flow when stall is used for power regulation at high wind speeds [19, 20].

Inaccurate predictions of wind turbine power and structural loads have led to insufficient design of wind turbine components, and premature failures. Some of the under predictions have been attributed to three-dimensional aerodynamic effects and dynamic stall. This delayed static stall produces much higher lift than predicted, resulting in an increase of turbine power and loading. For an airfoil oscillating or pitching through the static stall angle of attack, the onset of stall can be delayed to angles of attack considerably in excess of the static stall angle. However, when the airfoil does stall, the stall is more severe, and for oscillating airfoils, persists to lower angles of attack than the static stall. As the pitching airfoil passes through the static stall angle there is no discernible change in the viscous or inviscid flow about the airfoil. This is due to the finite time required for the stall events to occur. The first noticeable disturbance to occur is flow reversal in the boundary layer near the trailing edge. This flow reversal then proceeds toward the leading edge of the airfoil until flow reversal occurs over most of the chord. Large eddies appear in the boundary layer and a vortex forms near the leading edge. This vortex gains in strength, then convects over the airfoil. As the vortex moves across the airfoil the center of pressure moves with it causing a large nose-down pitching moment. After the vortex has passed the trailing edge, the airfoil experiences severe stall, with lift coefficient values often falling well below the static stall values. After full stall, as the angle of attack falls below the static stall value, the flow begins to reattach from front to rear, until unstalled values of aerodynamic force coefficients are again obtained [21].

At the present study an extensive wind tunnel tests have been carried to investigate the effects of various unsteady parameters on the pressure signature on the surface and behind a pitching airfoil. The airfoil is a section of a 660 kW horizontal axis wind turbine blade under construction in Iran. The velocity in the wake is measured using the pressure rake system and real time data acquisition. From these data, an estimation of profile and form drag in static and dynamic conditions is obtained.

II. Experimental Facility

All tests were conducted in the subsonic 0.8m×0.8m×2m closed circuit wind tunnel in Iran. The tunnel operates at speeds from 10 to 100 m/sec. A constant chord airfoil model was designed and manufactured for the test program. The model has 0.25m chord and 0.80m span and is the 16m section of a 660kW wind turbine blade.

The critical loading of the turbine blade occurs at this section. Fig. 1 shows the airfoil section along with the 64 pressure ports located on its upper and lower surfaces used for static and dynamic pressure measurements. The pressure ports are located along the chord at an angle of 20 degrees with respect to the model span to minimize disturbances from the upstream taps. Experiments show that the static stall angle of this 2D wing is about 11 degrees. For measuring the velocity profiles in the wake region, two pressure rakes are used as shown in Fig. 2. The shapes of both rakes are similar and one of them has 35 total pressure probes while the other one has 35 static pressure probes. The rakes are located at a distance of 1.5 chord length from the model trailing edge. The model is used in a section of a 660 kW horizontal axis wind turbine blade and was constructed from several layers of composite lay up of altering fiberglass and carbon fiber over ribs. After the production, it was digitized to ensure the true airfoil coordinate. Due to high number of pressure ports and size of the selected pressure transducers, we could not place the transducers inside the model. Therefore, extensive experiments were conducted to ensure that the time takes for the pressure to reach the transducers is much less than the frequency response of the transducers themselves, nominally 1 m sec. [22] and finally the tube length and material that gave minimum time lag for all applied pressures was selected. The pitch rotation point was fixed about the wing quarter chord. The oscillating system which is shown at Fig. 3 pitched the model at various amplitudes, means angles of attack, and reduced frequencies. The model angle of attack was varied sinusoidally as $\alpha = \alpha_{\circ} + \overline{\alpha}\sin(2\pi ft)$. Data were acquired and processed from surface pressure taps and rake ports, 2 individual tunnel pressure transducers, and an angle of attack encoder by means of two 12 bit, 64 channels National Instrument A/D Board capable of a sample rate of 500 kHz. Dynamic oscillatory data were then digitally filtered using low pass filter with various cut-off and transition frequencies to find the best frequencies to fit the original data. All oscillatory data presented here are an average of several cycles and were corrected for the solid tunnel sidewalls and the wake blockage effects [23]. Data were acquired at Reynolds numbers of 0.42, 0.63, and 0.84×10^{6}.

III. Results and Discussion

The primary purpose of the present study is to investigate the effect of unsteady parameters on the pressure signatures

and the wake of a sinusoidally oscillating airfoil of a 660 kW horizontal axis wind turbine blade. The pressure around the model is measured by the 64 ports located on the model. Furthermore, the velocity in the wake is determined by the use of pressure rake system and real time data acquisition.

To visualize the overall flow history on the airfoil surface and the wake, three dimensional illustrations of velocity profiles in the wake and pressure distributions on the airfoil surface are presented in Fig. 4. The sinusoidal high velocity defect result from the periodic movement of the trailing edge is seen. The velocity defect time history as shown in these figures closely follows the sinusoidal airfoil motion; however, when the oscillation amplitude is increased to 8 degrees, a very broad region of large velocity defect is noted, Fig. 4 (c) which is absent for the case of 2 and 5 degrees amplitude. This phenomenon is due to stall unset. On the other hand, pressure distribution on the airfoil both sides, upper and lower surfaces, shows sinusoidal variation when the oscillation amplitudes are 2 and 5 degrees. It is seen that variation is more obvious in the airfoil leading edge which shows that this airfoil has more sensitivity to flow field on its leading edge region. Fig. 4 (c) shows that with increasing the oscillation amplitude to 8 degrees, when $0.2<t/T<0.4$ pressure distribution carpet shows a region of pressure dropping which is established because of large amount of flow separation. This region is corresponded to the broad region of velocity defect on the wake flow history. The profile drag of a two-dimensional airfoil is the sum of the form drag due to boundary layer separation (pressure drag), and the skin friction drag. Usually the profile drag is determined from force measurement made using a mechanical balance attached to the model. In the two-dimensional case (where the airfoil spans the tunnel - wall to wall), the profile drag may also be determined from momentum considerations by comparing the velocity ahead of the model with that in its wake. This method is used here and momentum changes are derived from velocities obtained from two pressure rake. This technique is compromised because it requires the insertion of a physical body into the flow, resulting in a disturbance of the velocity field. Also it provides reasonable accuracy only in the low angles of attack range and in the absence of vortical structures in the wake. In the unsteady flow by neglecting the term that illustrates time variation of the momentum in the control volume, the linear momentum deficit can be calculated which is different from the usual profile drag coefficient which Ref. [24] has named this "drag indicator". In the present study, linear momentum deficit for both static and dynamic conditions named profile drag and compared with its corresponding form drag in various situations.

Fig. 5 shows the effects of oscillation amplitude on profile and form drag. It is seen by inspection that in static case up to $\alpha = 3\,\text{deg}$ the profile drag is greater than form drag. It is due to this fact that skin friction drag is dominant in this region. However, at higher angles of attack the form drag is higher due to the inaccuracies discussed later.

In dynamic situations the hysterises loops established almost around the static drag data. Moreover, form drag loops show that during upstroke phase of motion the dynamic drag is less than static one even at higher amplitudes its magnitude becomes negative. It is seen that with increasing of oscillation amplitude negative drag remains up to higher angles of attack. In addition, profile drag loops for dynamic case are quite near the static drag line at low angle of attack; thus we can conclude that the wake structure is independent of oscillating motion. For both dynamic form and profile drag the loops width increases with increasing of oscillating amplitude. Fig. 5 (c) shows that when the airfoil passes from its static stall angle the width of profile drag loop increases drastically and during downstroke motion its magnitudes are much higher than upstroke phase due to the large amount of flow separation during downstroke motion. This trend exists down to $\alpha = 4\,\text{deg}$.

The effect of reduced frequency is shown in Fig. 6. The overall effect of increasing the reduced frequency as seen from Fig. 6 is enhancing of the width of the hysteresis loops for both form and profile drag. However, form drag loops show an increase of their maximum magnitude and a decrease in their minimum value whether the dynamic angles of attack were lower or greater than the static stall angle. On the other hand, the profile drag hystersis loops show a decrease in maximum drag magnitude when the angle of attacks are above the static stall angle. This phenomenon is due to the increase of vortex strength and size shed into the wake.

Fig. 7 shows that the effect of increasing the Reynolds number on form and profile drag loops is similar to the reduced frequency effect, Fig. 6.

IV. Conclusion

Various tests were conducted in the wind tunnel to examine the dynamic form drag as well as profile drag on a model was undergoing pitching motion. The model was a section of a 660kw wind turbine blade. Tests were carried out with altering some important unsteady parameters that affecting the wind turbine performance such as reduced frequency and Re. It was found that the trend of form and profile drag is completely different at low and high angle of attack. Moreover, unsteady parameters, Re and reduced frequency had significant effect in their behavior.

Acknowledgment

This work was supported by the Iranian Renewable Energy Organization. Authors would like to thank their cooperation.

References

[1] McCroskey, W. J., "Unsteady Airfoils", Annual Rev. Fluid Mech. U.S. Army Aerodynamics Laboratory and NASA, pp. 285-309, 1982.
[2] Fan, Y., "Identification of an Unsteady Aerodynamic Model up to High Angle of Attack Regime," P.H.D Thesis, Virginia Polytechnic Institute and State University, 1997.
[3] Maresca, C., Favier, D., and Rebont, J., "Experiments on an airfoil at high angle of incidence in longitudinal oscillations", Journal of Fluid mechanics, vol.92, 1979, pp. 671-690.

[4] Broeren, A. P., and Bragg, M. B., “Spanwise variation in the unsteady stalling flowfields of two-dimensional airfoil models”., AIAA Journal , vol. 39 , no. 9 , Sept. , 2001, pp. 1641-1651.
[5] Walker, J. M., Helin H. E., and Chow, D. C. , B. E , “ Unsteady surfaces pressure measurement on a pitching airfoil” , AIAA-85-0532, AIAA Shear Flow Control Conference , March 12-14 , 1985.
[6] Peter Fuglsang, Ioannis Antoniou, Niels N. Sørensen, Helge Aa. Madsen, "Validation of a Wind Tunnel Testing Facility for Blade Surface Pressure Measurements," Risø-R-981(EN), 1998
[7] Carr, L. W., “Progress in Analysis and Prediction of Dynamic Stall,” Journal of Aircraft, Vol. 25, Jan 1988, pp. 6-17.
[8] McAlister, K. W., and Caw, L. W., "Water Tunnel Visualization of Dynamic Stall," Non steady Fluid Dynamics (ed. by Crow, P.E., and Miller, J. A.), p. 103, 1978.
[9] Satyanarayana, B., “Unsteady Wake Measurements of Airfoils and Cascades,” AIAA Journal, Vol. 15, May 1977, pp. 613-618.
[10] Jones, K.D., Dohring, C.M., and Platzer, M.F. "Wake Structures Behind Plunging Airfoils: A Comparison Of Numerical And Experimental Results," 34th Aerospace Sciences Meeting & Exhibit, AIAA 96−0078, 1996.
[11] Ho, C,-M. and Chen, S.-H. “Unsteady Wake of a Plunging Airfoil,” AIAA Journal, Vol.19, Nov. 1981, pp. 1492-1494.
[12] Park, S.O., Kim, J.S, Lee, B.I., “Hot-Wire Measurements of Near Wakes Behind an Oscillating Airfoil,” AIAA Journal Vol. 28, No. 1, 1989.
[13] Koochesfahani, M. M, “Vortical Patterns in the Wake of an Oscillating Airfoil,” AIAA Journal, Vol. 27, No. 9, Sep. 1989, pp. 1200-1205.
[14] Panda, J., and Zaman, K.B.M.Q “Experimental Investigation of the Flow Field of an Ocillating Airfol and Estimation of Lift from Wake Survays,” Journal of Fluid Mechanics, Vol. 265, 1994, pp. 65-95.
[15] Leishman, J. G., “Challenges in modeling the unsteady aerodynamics of wind turbines”, AIAA 2002-0037, 21st ASME Wind Energy Symposium and the 40th AIAA Aerospace Sciences Meeting , Jan. 14-17, 2002.
[16] Younsi, R., El-Batanong , I. Tritsch , J., Naji, H., and Landjerit, B., “Dynamic study of a wind turbine blade with horizontal axis” ,Sur. J. Mech. A/Solids 20, 2001, pp. 241-252.
[17] Huyer, S. A., Simms, D. A., and Robinson, M. C. , “Unsteady aerodynamics associated with a horizontal-axis wind turbine” , AIAA Journal , vol. 34, No. 7 , 1996 ,pp. 1410-1419.
[18] Hansen, A. C, Butterfield, C. P, "Aerodynamics of Horizontal -Axis Wind Turbines", Annul Rev. Fluid Mech. 1993.25:115, 1993.
[19] Gustave Paul Corten, "Flow Separation on Wind Turbine Blades"
[20] Tangler, Kocurek, J. D., "Wind Turbine Post-Stall Airfoil Performance Characteristics Guidelines for Blade-Element Momentum Methods", 43rd AIAA Aerospace Sciences Meeting and Exhibit, AIAA, 2005.
[21] Kirk Gee Pierce, "Wind Turbine Load Prediction Using The Beddoes-Leishman Model For Unsteady Aerodynamics And Dynamic Stall", Master of Science Thesis, The University of Utah, 1996
[22] Soltani, M. R., Rasi, F., Seddighi, M., and Bakhshalipour, A.“An Experimental Investigation of Time lage in Pressure Measuring System” , Ankara International Aerospace Conference, Turkey, 2005.
[23] Rae, W. H., and Pope, A. , Low Speed Wind Tunnel Testing, Second edition, John Wiley and Sons, 2000.
[24] Satyanarayana B. and C. S. Lee “Unsteady Wake Measurements of an Oscillating Flap at Transonic Speeds,” AIAA Journal, Vol. 24, No. 12, 1986.

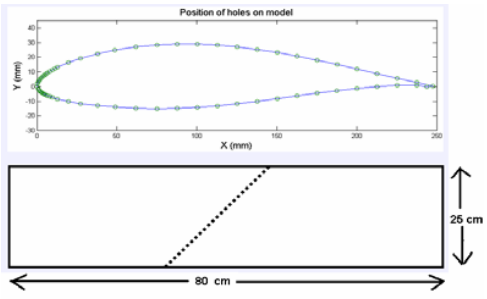

Fig. 1 Airfoil section and location of pressure ports

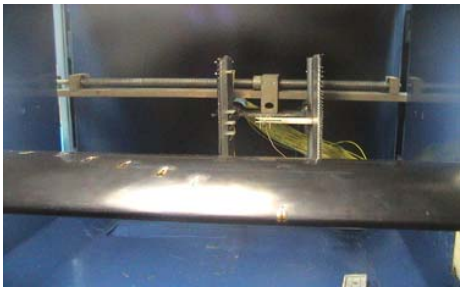

Fig. 2 Static and Total Pressure Rakes

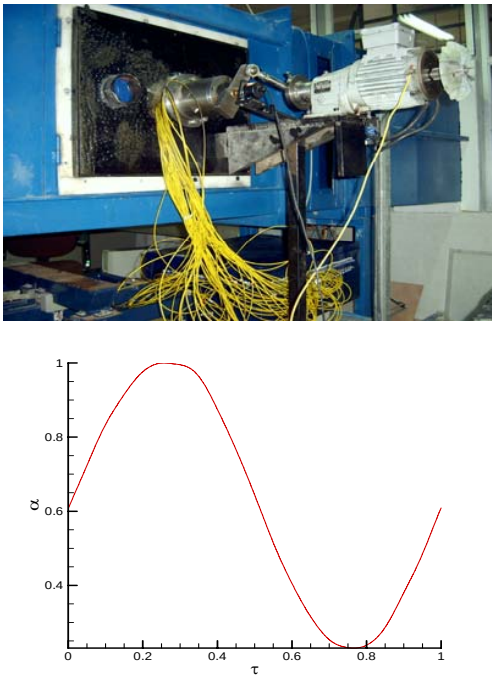

Fig. 3 Pitching Oscillation System and a typical angle of attack history of the model

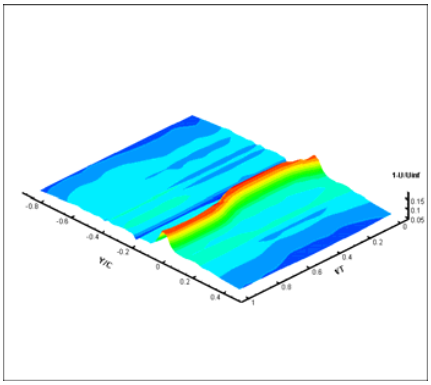

Wake velocity

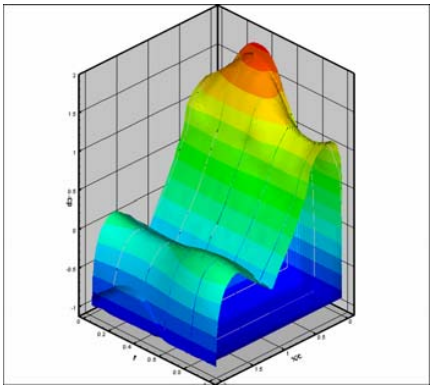

Surface pressure

(a) $\alpha_0 = 5\deg$, $\overline{\alpha} = 2\deg$, $U_\infty = 60$ m/s, $k = 0.024$

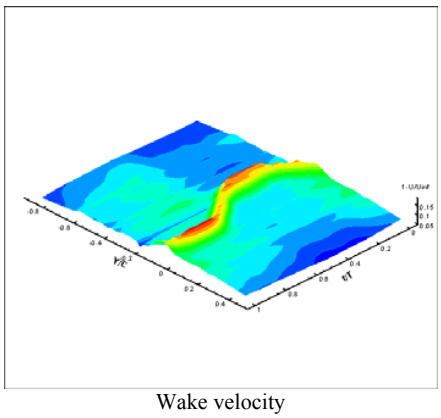

Wake velocity

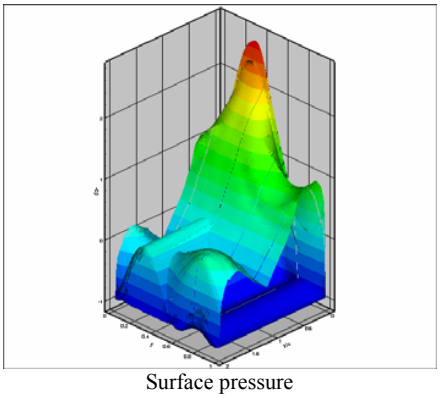

Surface pressure

(b) $\alpha_0 = 5\deg$, $\overline{\alpha} = 5\deg$, $U_\infty = 60$ m/s, $k = 0.024$

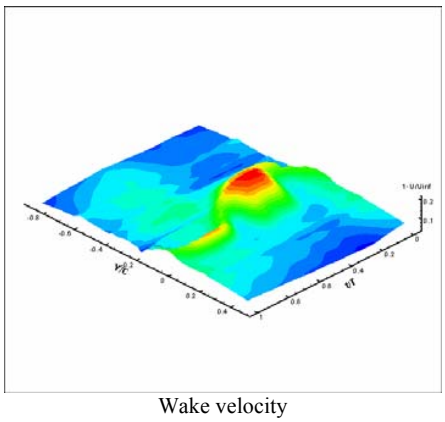

Wake velocity

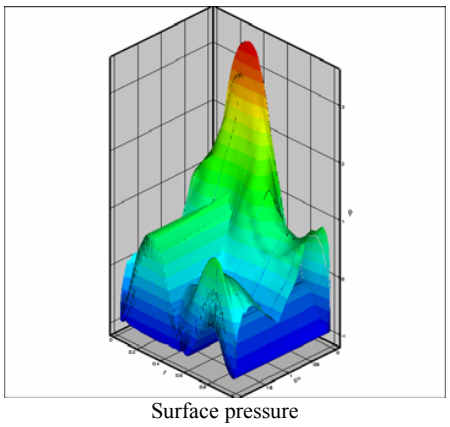

Surface pressure

(c) $\alpha_0 = 5\deg$, $\overline{\alpha} = 8\deg$, $U_\infty = 60$ m/s, $k = 0.024$

Fig. 4 Wake velocity and pressure field on the airfoil surface

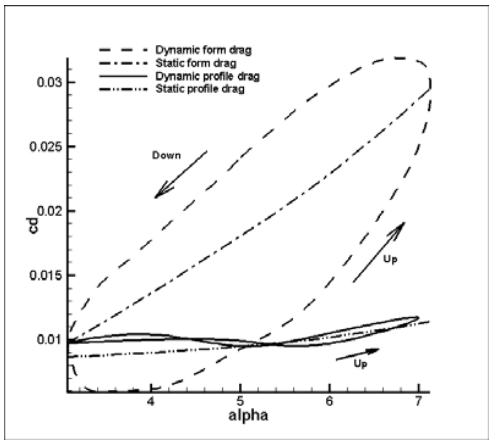

(a) $\alpha_0 = 5\deg$, $\bar{\alpha} = 2\deg$, $U_\infty = 60$ m/s, $k = 0.024$

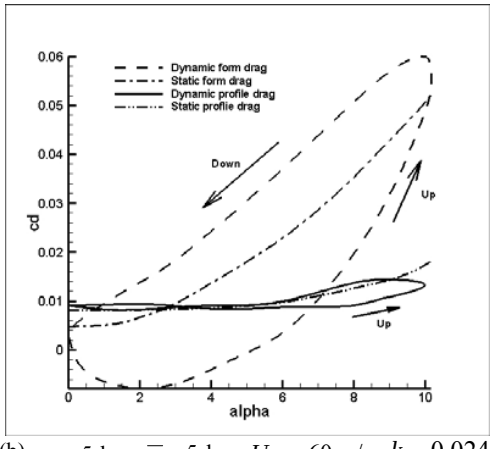

(b) $\alpha_0 = 5\deg$, $\bar{\alpha} = 5\deg$, $U_\infty = 60$ m/s, $k = 0.024$

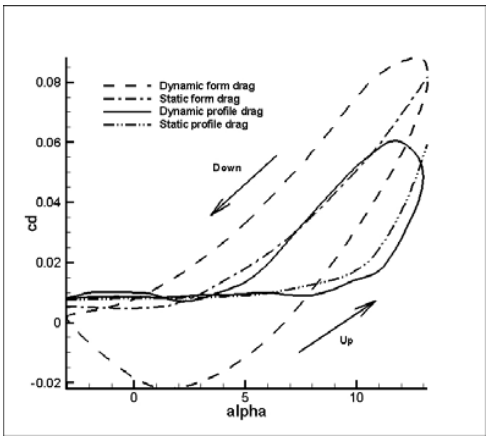

(c) $\alpha_0 = 5\deg$, $\bar{\alpha} = 8\deg$, $U_\infty = 60$ m/s, $k = 0.024$

Fig. 5 Amplitude effect on dynamic form and profile drag and static drag coefficient

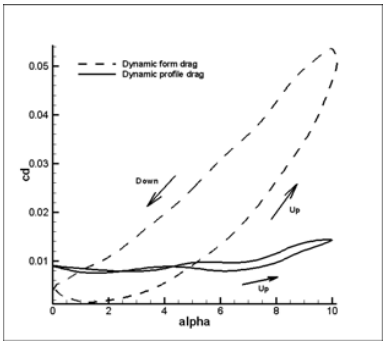

$\alpha_0 = 5\text{deg},\ \overline{\alpha} = 5\text{deg},\ U_\infty = 60\ \text{m/s},\ k = 0.013$

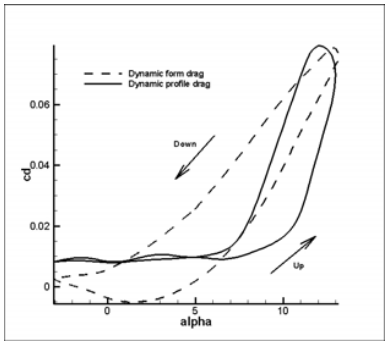

$\alpha_0 = 5\text{deg},\ \overline{\alpha} = 8\text{deg},\ U_\infty = 60\ \text{m/s},\ k = 0.013$

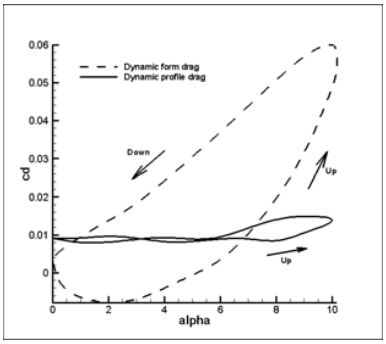

$\alpha_0 = 5\text{deg},\ \overline{\alpha} = 5\text{deg},\ U_\infty = 60\ \text{m/s},\ k = 0.024$

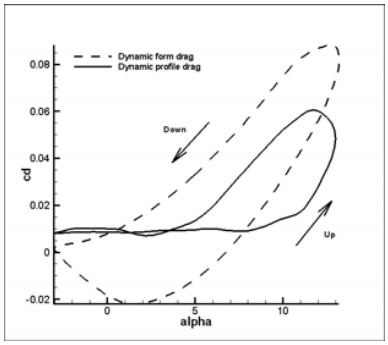

$\alpha_0 = 5\text{deg},\ \overline{\alpha} = 8\text{deg},\ U_\infty = 60\ \text{m/s},\ k = 0.024$

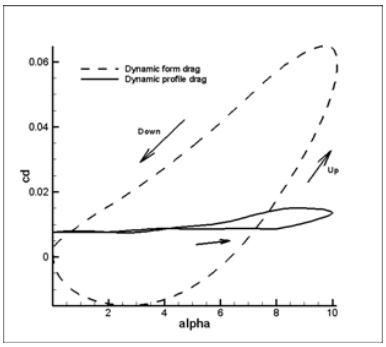

$\alpha_0 = 5\text{deg},\ \overline{\alpha} = 5\text{deg},\ U_\infty = 60\ \text{m/s},\ k = 0.03$

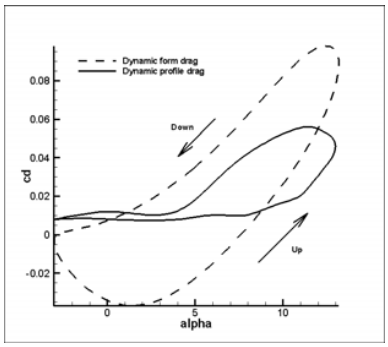

$\alpha_0 = 5\text{deg},\ \overline{\alpha} = 8\text{deg},\ U_\infty = 60\ \text{m/s},\ k = 0.03$

Fig. 6 Effect of reduced frequency on form and profile drag loops

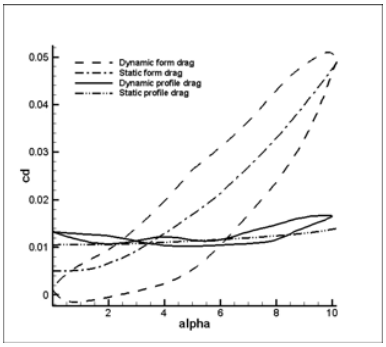

$\alpha_0 = 5\deg,\ \overline{\alpha} = 5\deg,\ k = 0.03,\ \mathrm{Re} = 0.42\times10^6$

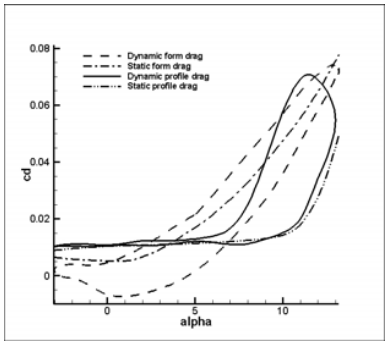

$\alpha_0 = 5\deg,\ \overline{\alpha} = 8\deg,\ k = 0.03,\ \mathrm{Re} = 0.42\times10^6$

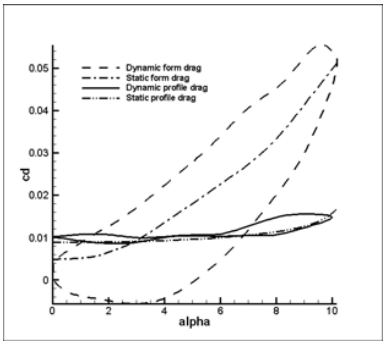

$\alpha_0 = 5\deg,\ \overline{\alpha} = 5\deg,\ k = 0.03,\ \mathrm{Re} = 0.63\times10^6$

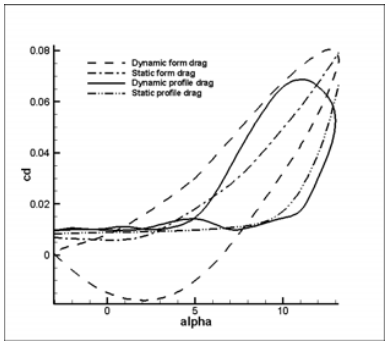

$\alpha_0 = 5\deg,\ \overline{\alpha} = 8\deg,\ k = 0.03,\ \mathrm{Re} = 0.63\times10^6$

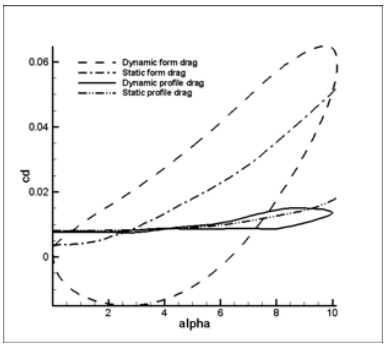

$\alpha_0 = 5\deg,\ \overline{\alpha} = 5\deg,\ k = 0.03,\ \mathrm{Re} = 0.84\times10^6$

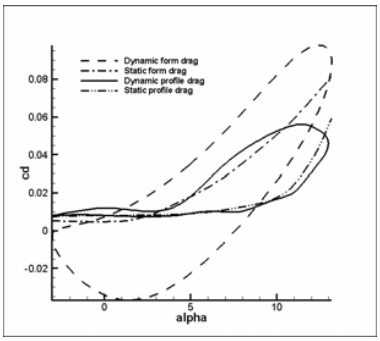

$\alpha_0 = 5\deg,\ \overline{\alpha} = 8\deg,\ k = 0.03,\ \mathrm{Re} = 0.84\times10^6$

Fig. 7 Effect of Reynolds number on form and profile drag loops